

## On Direct Verification of Warped Hierarchy-and-Flavor Models

Hooman Davoudiasl,<sup>1,\*</sup> Thomas G. Rizzo<sup>†,2,‡</sup> and Amarjit Soni<sup>1,§</sup>

<sup>1</sup>*Department of Physics, Brookhaven National Laboratory, Upton, NY 11973-5000, USA*

<sup>2</sup>*Stanford Linear Accelerator Center,*

*2575 Sand Hill Rd., Menlo Park, CA 94025, USA*

### Abstract

We consider direct experimental verification of warped models, based on the Randall-Sundrum (RS) scenario, that explain gauge and flavor hierarchies, assuming that the gauge fields and fermions of the Standard Model (SM) propagate in the 5D bulk. Most studies have focused on the bosonic Kaluza Klein (KK) signatures and indicate that discovering gauge KK modes is likely possible, yet challenging, while graviton KK modes are unlikely to be accessible at the LHC, even with a luminosity upgrade. We show that direct evidence for bulk SM fermions, *i.e.* their KK modes, is likely also beyond the reach of a luminosity-upgraded LHC. Thus, neither the spin-2 KK graviton, the most distinct RS signal, nor the KK SM fermions, direct evidence for bulk flavor, seem to be within the reach of the LHC. We then consider hadron colliders with  $\sqrt{s} = 21, 28,$  and  $60$  TeV. We find that discovering the first KK modes of SM fermions and the graviton typically requires the Next Hadron Collider (NHC) with  $\sqrt{s} \approx 60$  TeV and  $\mathcal{O}(1)$   $\text{ab}^{-1}$  of integrated luminosity. If the LHC yields hints of these warped models, establishing that Nature is described by them, or their 4D CFT duals, requires an NHC-class machine in the post-LHC experimental program.

*Submitted to Physical Review D*

---

<sup>†</sup> Work supported in part by the Department of Energy, Contract DE-AC02-76SF00515.

\*Electronic address: hooman@bnl.gov

<sup>‡</sup>Electronic address: rizzo@slac.stanford.edu

<sup>§</sup>Electronic address: soni@bnl.gov

## I. INTRODUCTION

The Randall-Sundrum (RS) model [1] was originally proposed to resolve the hierarchy between the scales of weak and gravitational interactions,  $m_W \sim 10^2$  GeV and  $\bar{M}_P \sim 10^{18}$  GeV, respectively. The RS model is based on a truncated AdS<sub>5</sub> spacetime, bounded by two 4D Minkowski walls, often called UV (Planck) and IR (TeV) branes. The curvature in 5D induces a warp factor in the metric which redshifts scales of order  $\bar{M}_P$  at the UV brane to scales of order  $m_W$  at the IR brane. Since the metric depends exponentially on the 5<sup>th</sup> coordinate, explaining  $m_W/\bar{M}_P \sim 10^{-16}$  does not require hierarchic parameters. The requisite brane-separation was shown to be easily accommodated early on [2].

Initially, it was assumed that all Standard Model (SM) fields reside at the IR brane. The most striking and distinct signature of this model would then be weak scale spin-2 Kaluza-Klein (KK) excitations of the graviton, appearing as resonances in high energy collisions [3]. It was soon realized that resolving the hierarchy only required the Higgs to be localized near the IR brane [4] and SM gauge [5, 6] and fermion [7] fields could propagate in the 5D bulk. It was shown that placing the fermions in the bulk provides a natural mechanism for generation of SM fermion masses and also suppression of unwanted 4-fermion operators [8]. This is achieved by a mild modulation of bulk fermion masses that control the exponential localization of fermion zero modes. As the Higgs is kept near the IR brane, small 4D Yukawa couplings are naturally obtained, if light flavor zero modes are UV brane localized. Given the correspondence between location in the bulk and scale in warped backgrounds, operators containing light flavors are suppressed by scales much larger than  $m_W$ .

The above setup, an RS-type geometry with a flavored bulk, offers an attractive simultaneous resolution of hierarchy and flavor puzzles. However, the experimental signals of these warped models are now much more elusive. This is because spreading the gauge fields over the bulk and localizing the light fermions near the UV brane suppresses their couplings to IR-brane-localized KK modes, the main signatures of warped models. Therefore, their production via and decay into light SM fermions and gauge fields are suppressed. This feature is generic to warped models of hierarchy and flavor, largely independently of their details.

Recently, various studies have been performed to assess the prospects for discovering the new warped scenarios, given that the old set of signatures are now mostly inaccessible. Precision data require the new KK states to be heavier than roughly 2-3 TeV [9], even

assuming new custodial symmetries [16]. Generally speaking, it has been shown that the most likely new state in these models to be discovered at the LHC is the first KK gluon [17, 18]. The analysis of Refs. [17, 18] suggests that KK gluons as heavy as 4 TeV will be within the reach of the LHC. However, for the KK modes of the weak sector, the corresponding reach is in the 2-3 TeV range [19]. For gauge KK masses in the above ranges, the graviton KK modes are most likely not accessible, even with an upgraded LHC luminosity [20, 21]. Thus, typically, the gauge KK modes may be discovered, while the KK gravitons which are the most distinct RS-type signature will be out of reach, at the LHC.

In this work, we examine the discovery prospects for the KK modes of the SM fermion sector. Observation of these states will provide direct evidence for the presence of SM fermions in the 5D bulk, a necessary ingredient of the warped flavor scenarios. Briefly put, we find that with gauge KK masses set at 3 TeV, a currently acceptable value, and for generic zero-mode profiles that yield a realistic flavor hierarchy, the SM KK fermions are not accessible at the LHC, even after a luminosity upgrade. Hence, we are faced with a situation in which the KK modes of the graviton and SM fermions are not discovered during the LHC program. However, it seems reasonable to require direct observation of these KK states in order to establish an RS-type warped model as a theory of hierarchy and flavor.

Given our conclusion that the LHC is unlikely to establish realistic warped models, we set out to determine the minimum requirements that a future machine needs to meet in order to make this task possible. We take 3 TeV to be a reference mass for the lowest gauge KK mode. This sets the mass scales of all other KK states, in the simplest generic warped models. What we find is that, typically, in order to have firm evidence for the lowest KK states with spins 1/2, 1, and 2, we need center of mass energies  $\sqrt{s} \approx 60$  TeV and integrated luminosities  $L \sim 1 \text{ ab}^{-1}$ . This suggests that future *luminosity and energy* upgrades of the LHC will most likely be insufficient to verify all the essential features of realistic warped models. Therefore, if these models do describe Nature, the LHC will likely find evidence for them. However, the Next Hadron Collider (NHC), defined to have  $\sqrt{s} \approx 60$  TeV and  $L \sim 1 \text{ ab}^{-1}$ , must be part of the post-LHC experimental program aimed at establishing the underlying theory. We also show that if these states are not observed at the LHC the eventual reach of NHC for the gluon KK states is typically in excess of 10 TeV.

In the next section we review key aspects of typical Warped Hierarchy-and-Flavor Models (WHFM). In section 3, we study the prospects for verification of realistic WHFM at colliders

and estimate the required parameters of the NHC. Our conclusions are presented in section 4.

## II. WARPED HIERARCHY-AND-FLAVOR MODELS

Here, we will briefly describe the generic properties of WHFM. Much of what will follow is well-known from previous works and is mainly included to provide some background for our further discussions.

### A. General Features

The RS metric is given by [1]

$$ds^2 = e^{-2\sigma} \eta_{\mu\nu} dx^\mu dx^\nu - r_c^2 d\phi^2, \quad (1)$$

where  $\sigma = kr_c|\phi|$ ,  $k$  is the 5D curvature scale,  $r_c$  is the radius of compactification,  $-\pi \leq \phi \leq \pi$ , and a  $\mathbb{Z}_2$  orbifolding of the 5<sup>th</sup> dimension is assumed.

To solve the hierarchy problem, the Higgs is assumed to be localized near the TeV-brane, where the reduced metric “warps”  $\langle H \rangle_5 \sim \bar{M}_P$  down to the weak scale:  $\langle H \rangle_4 = e^{-kr_c\pi} \langle H \rangle_5$ . For  $kr_c \approx 11.3$ , we then get  $\langle H \rangle_{\text{SM}} \equiv \langle H \rangle_4 \sim 100$  GeV. Originally, it was assumed that all SM content resides at the IR-brane [1]. However, as the cutoff scale in the 4D effective theory is also red-shifted to near the weak-scale, this would lead to unsuppressed higher dimensional operators that result in large violations of experimental bounds on various effects, such as those on flavor-changing neutral currents. This problem can be solved by realizing that points along the warped 5<sup>th</sup> dimension correspond to different effective 4D scales. In particular, by localizing first and second generation fermions away from the IR-brane, the effective scale that suppresses higher dimensional operators made up of these fields is pushed to much higher scales [8]. In the process of suppressing the dangerous operators, this setup also leads to a natural mechanism for obtaining small fermion masses.

The above localization is achieved by introducing a 5D mass term in the bulk for each fermion field  $\Psi$  [7]. Let  $c \equiv m_\Psi/k$ , where  $m_\Psi$  is the 5D mass of the fermion. Each 5D fermion  $\Psi$  has left- and right-handed components  $\Psi_{L,R}$  which can be expanded in KK modes

$$\Psi_{L,R}(x, \phi) = \sum_{n=0}^{\infty} \psi_{L,R}^{(n)}(x) \frac{e^{2\sigma}}{\sqrt{r_c}} f_{L,R}^{(n)}(\phi). \quad (2)$$

The KK wavefunctions  $f_{L,R}^{(n)}$  are orthonormalized

$$\int d\phi e^\sigma f_{L,R}^{(m)} f_{L,R}^{(n)} = \delta_{mn}. \quad (3)$$

One can then show that the  $n \neq 0$  modes are given by [7]

$$f_{L,R}^{(n)} = \frac{e^{\sigma/2}}{N_n^{L,R}} Z_{\frac{1}{2} \pm c}(z_n), \quad (4)$$

where the normalization  $N_n^{L,R}$  is fixed by Eq.(3); throughout our work,  $Z_a = J_a + b_n Y_a$  denotes a linear combination of Bessel functions of order  $a$ . In Eq.(4),  $z_n \equiv (m_n/k)e^\sigma$  and  $m_n$  is the KK mass. The zero-mode wavefunction is given by

$$f_{L,R}^{(0)} = \frac{e^{\mp c\sigma}}{N_0^{L,R}}, \quad (5)$$

with the normalization

$$N_0^{L,R} = \left[ \frac{e^{kr_c\pi(1 \mp 2c)} - 1}{kr_c(1/2 \mp c)} \right]^{1/2}. \quad (6)$$

Note that in our convention, the singlet (right-handed) and doublet (left-handed) zero mode wavefunctions are defined with opposite signs for mass parameters  $c^S$  and  $c^D$ , respectively. Hence, for example, UV-localization for the singlet and doublet zero modes correspond to  $c^S < -1/2$  and  $c^D > 1/2$ , respectively.

In the SM, all  $SU(2)$  doublets are left-handed, while the singlets are right-handed. One can impose a  $\mathbb{Z}_2$  parity on bulk fermion fields so that only the doublets have left-handed zero modes and only the singlets have right-handed zero modes. However, both the doublets and singlets have left- and right-handed higher KK modes. To project a particular 4D zero mode chirality, Neumann-like boundary conditions are chosen for the corresponding field at  $\phi = 0, \pi$ ; the other chirality will then obey Dirichlet boundary conditions. For example, if  $\Psi^D$  represents a weak SM doublet, we require

$$(\partial_\phi + r_c m_\Psi) f_L^{(n)} = 0 \quad ; \quad f_R^{(n)} = 0 \quad \text{at } \phi = 0, \pi. \quad (7)$$

The above choice results in a left-handed zero mode, given by Eq.(5). We also find

$$b_n^{L,R} = -\frac{J_{\pm(c-1/2)}(z_n)}{Y_{\pm(c-1/2)}(z_n)} \quad \text{at } \phi = 0, \pi. \quad (8)$$

The above equations fix the wavefunctions and the mass eigenvalues, once  $c$  is specified for any  $SU(2)$  doublet  $\Psi^D$ ;  $(L, R)$  equations result in the same KK mass spectrum. Similar equations can also be derived for singlets  $\Psi^S$ .

The above fermion profiles lead to a natural scheme for SM fermion masses [7, 8]. We will assume that the Higgs is on the IR-brane; this is a very good approximation since the Higgs must be highly IR-localized. Then, a typical Yukawa term in the 5D action will take the form

$$S_Y^5 = \int d^4x d\phi \sqrt{-g} \frac{\lambda_5}{k} H(x) \Psi_L^D \Psi_R^S \delta(\phi - \pi), \quad (9)$$

where  $\lambda_5 \sim 1$  is a dimensionless 5D Yukawa coupling and  $\Psi^{D,S}$  are doublet left- and singlet right-handed 5D fermions, respectively. After the rescaling  $H \rightarrow e^{kr_c\pi} H$ , the 4D action resulting from Eq.(9) is

$$S_Y^4 = \int d^4x \sqrt{-g} \lambda_4 H(x) \psi_L^{(D,0)} \psi_R^{(S,0)} + \dots, \quad (10)$$

where the 4D Yukawa coupling for the corresponding zero-mode SM fermion is given by [8]

$$\lambda_4 = \frac{\lambda_5}{kr_c} \left[ \frac{e^{(1-c^D+c^S)kr_c\pi}}{N_0^{D,L} N_0^{S,R}} \right], \quad (11)$$

Thus, in the quark sector, there are, in general, 9 different values for  $c^{D,S}$ : 3 for the doublets and 6 for the singlets. One can see that the exponential form of the effective Yukawa coupling  $\lambda_4$  can accommodate a large hierarchy of values without the need for introducing unnaturally small 5D parameters.

With the fermions in the bulk, the gauge fields must also follow. A 5D gauge field  $A_M$  has scalar and vector projections in 4D. The scalar zero mode corresponding to  $A_\phi$  is projected out using  $\mathbb{Z}_2$  parity or a Dirichlet boundary condition. As is well-known, the remaining projections  $A_\mu$  can be expanded in KK modes as

$$A_\mu = \sum_{n=0}^{\infty} A_\mu^{(n)}(x) \frac{\chi^{(n)}(\phi)}{\sqrt{r_c}}. \quad (12)$$

The gauge field KK wavefunctions are given by [5, 6]

$$\chi_A^{(n)} = \frac{e^\sigma}{N_n^A} Z_1(z_n) \quad (13)$$

subject to the orthonormality condition

$$\int_{-\pi}^{\pi} d\phi \chi_A^{(m)} \chi_A^{(n)} = \delta_{mn}. \quad (14)$$

The above equation fixes the normalization  $N_n^A$  and Neumann boundary conditions at  $\phi = 0, \pi$  fix the wavefunctions and yield the KK masses.

The 5D action for the coupling of the bulk fermion  $\Psi$  to the gauge field  $A_M$  is given by

$$S_{\Psi A} = g_5 \int d^4x d\phi V [V_l^M \bar{\Psi} \gamma^l A_M \Psi], \quad (15)$$

where  $g_5$  is the 5D gauge coupling,  $V$  is the determinant of the fünfbein  $V_l^M$ , with  $l = 0, \dots, 3$ ,  $V_\lambda^M = e^\sigma \delta_\lambda^M$ , and  $V_4^4 = -1$ ;  $\gamma^l = (\gamma^\lambda, i\gamma^5)$ . Dimensional reduction of the action (15) then yields the couplings of the fermion and gauge KK towers. With our conventions, the 4D gauge coupling is given by  $g_4 = g_5/\sqrt{2\pi r_c}$ , which fixes the couplings of all the other modes.

For completeness, we also write down the wavefunction of the graviton KK modes [3]

$$\chi_G^{(n)} = \frac{e^{2\sigma}}{N_n^G} Z_2(z_n) \quad (16)$$

which obey Neumann boundary conditions and are orthonormalized according to

$$\int_0^\pi d\phi e^{-2\sigma} \chi_G^{(m)} \chi_G^{(n)} = \delta_{mn}. \quad (17)$$

The graviton wavefunctions are fixed and the corresponding KK masses are obtained, via the boundary conditions, as before.

WHFM are subject to various experimental constraints, including those from precision electroweak [9] and flavor data [10, 11]. A number of models with a custodial  $SU(2)_L \times SU(2)_R$  bulk symmetry have been proposed to address these constraints [12, 13, 14]. In the following, we will limit the scope of our study to bulk SM without specifying a particular framework for such constraints. We will not discuss the phenomenology of the extra exotica in these models, as they do not change the qualitative picture for the SM KK partners that we present here. This will suffice to demonstrate our key observations. For a study of possible light exotic quarks in some warped scenarios see Ref. [15].

## B. Reference Parameters

To comply with precision constraints, we will choose the mass of the first KK mode of gauge fields to be 3 TeV [9]. This implies that we have assumed extra custodial symmetries, as explained in the above. We ignore brane localized kinetic terms for various bulk fields, as they are most naturally loop suppressed. Then, the RS geometry fixes the ratios of all KK masses. In what follows, we will also ignore potential mixing among various KK modes that can induce small shifts in their masses. These considerations do not change our main

conclusions regarding discovery reach for WHFM, at colliders. The masses of various KK modes are given by

$$m_n = x_n k e^{-kr_c \pi}, \quad (18)$$

where for gauge fields  $x_n = 2.45, 5.56, 8.70, \dots$  and for the graviton  $x_n^G = 3.83, 7.02, 10.17, \dots$

The values of KK masses for SM fermions depends on the bulk mass parameter  $c$ . In the fermion sector, we will only discuss the reach for SM KK quarks, since we will concentrate on multi-TeV hadron colliders. Here, we choose  $c^D \approx -c^S \approx 0.6$  for *light* quarks. This choice results in masses of order 10-100 MeV for  $\mathcal{O}(1)$  bulk Yukawa couplings. This range roughly covers the quark flavors ( $u, d, s$ ) which constitute the dominant quark initial states for collider production of new physics. It turns out that the KK modes of all quarks, except for the singlet top quark, are roughly degenerate in mass with KK modes of the gauge fields. To get a reasonable top quark mass, we choose  $c_t^D \approx c_t^S \approx 0.4$ , giving a singlet top first KK mass roughly 1.5 times the first gauge KK mass.

To assess the relative significance of various production channels, we must know the relevant couplings that enter the calculations (an earlier qualitative discussion in a somewhat different context can be found in Ref.[23]). Again, we only discuss typical values to keep our discussion more general and less parameter-specific. We adopt the notation  $g_{mn}^l$  to denote the coupling of the  $l^{\text{th}}$  gauge KK mode to fermions of the  $m^{\text{th}}$  and  $n^{\text{th}}$  KK levels;  $g_{00}^0 \equiv g_{SM}$ . We will focus on the gluon and quark sectors, so  $g_{SM} = g_s$ , the strong coupling constant.

First, we will consider single production of KK quarks. This cannot proceed via fusion of quark and gluon zero modes, since this vertex is zero by orthogonality of fermion KK wavefunctions. Next, is the possibility of production in association with a zero mode quark. The gluon-mediated diagram again gives zero, by orthogonality. However, KK-gluon-mediation gives a non-zero result. Given that KK gluons are IR-localized, the only feasible channels involve the third generation zero modes. We find that the coupling  $g_{00}^1 \sim g_s/5$ , for light quarks. Note that the initial states cannot be gluons, by orthogonality of the gluon KK modes. For  $(t, b)_L$  and  $t_R$ , we get  $g_{01}^1 \sim \sqrt{2\pi} g_s$ . Hence, production in these channels is roughly proportional to  $(\sqrt{2\pi} g_s^2/5)^2 \sim g_s^4/4$ . Given that the KK modes of the singlet top are about 1.5 heavier than the doublets, the most promising channel is single production of a third generation doublet KK mode in association with a  $t$  or a  $b$ .

Next, let us examine pair production of KK quarks. Gluon mediated production can come from zero mode quark and gluon initial states; each of these amplitudes is proportional to  $g_s^2$ .



There is also a KK gluon mediated channel. Here, the amplitude is roughly proportional to  $g_s^2$ ; this is due to an approximate cancellation of volume suppression and enhancement at the two vertices for this process. Therefore, we see that pair-production has a number of SM-strength channels available to it, unlike the single production. This can offset the kinematic suppression from producing two heavy states. In fact we will later see that pair-production will dominate single-production with our typical choices of parameters.

Finally, since we will also discuss discovery reach for KK gravitons, we will briefly review their relevant couplings. As is well-known, light quark zero modes have a negligible coupling to KK gravitons. This is because of the extreme IR-localization of these KK gravitons, compared with KK gauge fields. Thus, in generic WHFM, only the coupling  $C_{00n}^{AAG}$  of two gluons to the KK graviton is important for its collider production [20, 21]. In units of the graviton zero mode coupling,  $1/\bar{M}_P$ , we have [22]

$$C_{00n}^{AAG} = e^{kr_c\pi} \frac{2 [1 - J_0(x_n^G)]}{kr_c\pi (x_n^G)^2 |J_2(x_n^G)|}, \quad (19)$$

where the first few  $x_n^G$  were given above.

### III. EXPERIMENTAL PROSPECTS FOR VERIFICATION OF WHFM

Given the discussion in the previous section, the first thing we need to do is to demonstrate that single (associated) production of KK fermions together with their corresponding zero modes is relatively suppressed in comparison to the production of KK fermion pairs. We will concentrate on the quark and gluon sectors. This reaction is dominated by the subprocess  $q\bar{q} \rightarrow g^{(1)} \rightarrow q^{(1)}\bar{q}^{(0)} + h.c.$ , where the first gluon KK mode  $g^{(1)}$  is somewhat off-shell. (We assume the width to mass ratio of this gluon KK to be 1/6 in our analysis, following Ref. [17].) To be concrete, we focus our attention on the excitations of the left-handed third generation quark doublet  $Q_3 = (t, b)_L^T$  since it has a large coupling to  $g^{(1)}$ , as discussed above.

For the LHC, the results of these calculations for single production can be seen in Fig. 1 while generalization to higher energy colliders can be seen in Fig. 2. Note that no cuts or branching fractions have been included in these calculations, in order to avoid a model-specific analysis. These rates will go down if we assume a more massive gluon KK state. In this work, we will generally assume that  $\mathcal{O}(100)$  events will be sufficient to establish the discovery of a KK mode. The results in Figs. (1) and (2) represent the case with the product

of the entrance and exit channel couplings equal to  $g_s^2$ , the SM value. However, from our discussion in the previous section, we expect that a more realistic value, for these processes, is  $g_s^2/2$ , suppressing the production by factor of about 4. The rates, as can be seen from the figures, are not very impressive, even with this optimistic assumption. It is clear that this process will be unobservable at the LHC even with a luminosity upgrade. Further, note that the cross section only increases by a factor of order  $\sim 20$  in the peak region when going from  $\sqrt{s} = 14$  to 60 TeV.

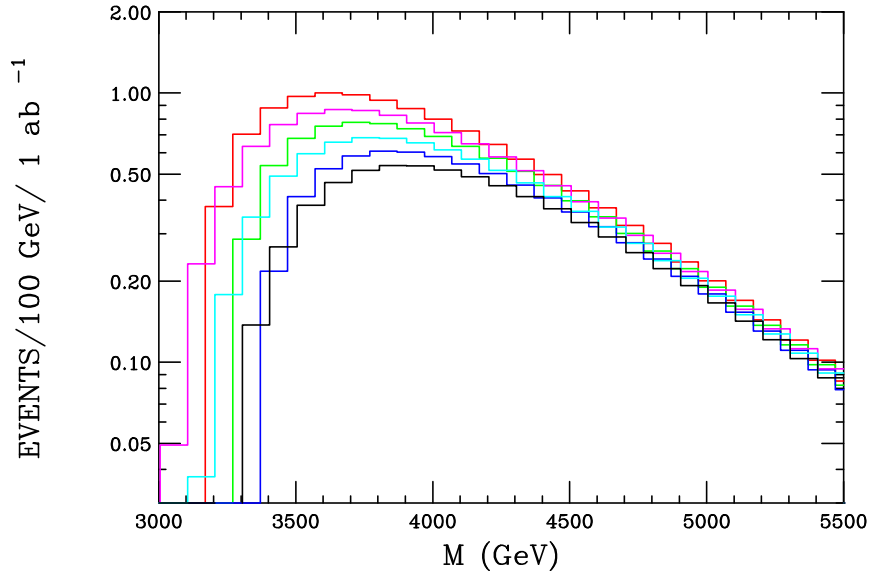


FIG. 1: Rates for the associated production of first  $t_L$  and  $b_L$  KK excitations together with their corresponding zero modes at the LHC; the results for  $t(b)_L$  correspond to to the higher (lower) member of each histogram pair, respectively. Here the first gluon KK mass is fixed at 3 TeV and we show the results as a function of the fermion pair mass. The three sets of histograms assume that the  $b_L$  KK mass is 100 (200, 300) GeV heavier than the gauge KK whereas the threshold for  $t_L$  is somewhat higher due to the larger zero mode top mass.

We now turn to the possibility of fermion KK pair production which can arise from both  $q\bar{q}$  and  $gg$  initial states as discussed above and is mediated by the entire gluon KK tower, including the zero mode. (Note that in our calculations we include only the first three gluon KK excitations as well as the SM gluon.) The results of these calculations are shown in Fig. 3 and 4 with no cuts or branching fractions applied. Again we see that for the LHC the rates are far too small to be useful but they grow quite rapidly as the collider energy increases; without much effort we see that  $\sqrt{s} = 28$  GeV is perhaps the bare minimum

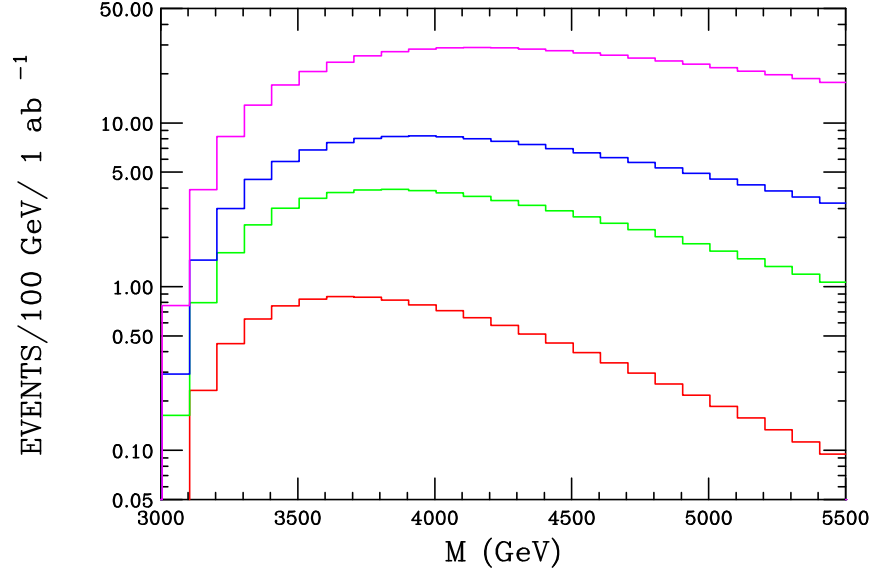


FIG. 2: Same as the last figure but now for different values of  $\sqrt{s}$  and taking the first gluon KK and fermion KK masses to be degenerate at 3 TeV. From bottom to top the histograms correspond to  $\sqrt{s} = 14, 21, 28$  and  $60$  TeV, respectively.

requirement to observe these KK states and an even higher value is likely to be necessary if efficiencies and branching fractions are suitably accounted for.

We will now discuss the likely dominant decay channels for KK quarks, without entering into a detailed analysis. We will consider the gauge eigen-basis picture, for simplicity. Given that the KK quarks are somewhat heavier than the gluon KK modes,  $q_{KK} \rightarrow q g_{KK}$ , with  $q$  a zero-mode quark, is a possible decay channel; let us denote this possibility as channel A. Another potentially important decay mode is through the brane-localized Yukawa coupling to the Higgs:  $q_{KK}^i \rightarrow H q_{KK}^j$  where the final quark KK mode is lighter than the one in the initial state; we will refer to this as channel B. Channel C in the following will refer to  $q_{KK}^i \rightarrow H q^j$  with  $q^j$  denoting another zero-mode quark. (The weak-sector analog of channel A will be suppressed by the weak coupling constant so we will ignore it in the discussion which follows.) Note that here if  $q^i$  is a weak doublet then  $q^j$  is a weak singlet, and vice versa. The subsequent decay of the gluon KK state in channel A produces the final state  $q t \bar{t}$ . In channel B, depending on whether  $q_{KK}^j$  decays through channels A or C, we get either  $H q t \bar{t}$  or  $H H q$ , respectively as a final state.

The couplings in channels A and C are controlled by the overlap of the zero mode quark with the IR brane states,  $g_{KK}$  or  $H$ . For channel B this coupling is  $\mathcal{O}(1)$ , when allowed,

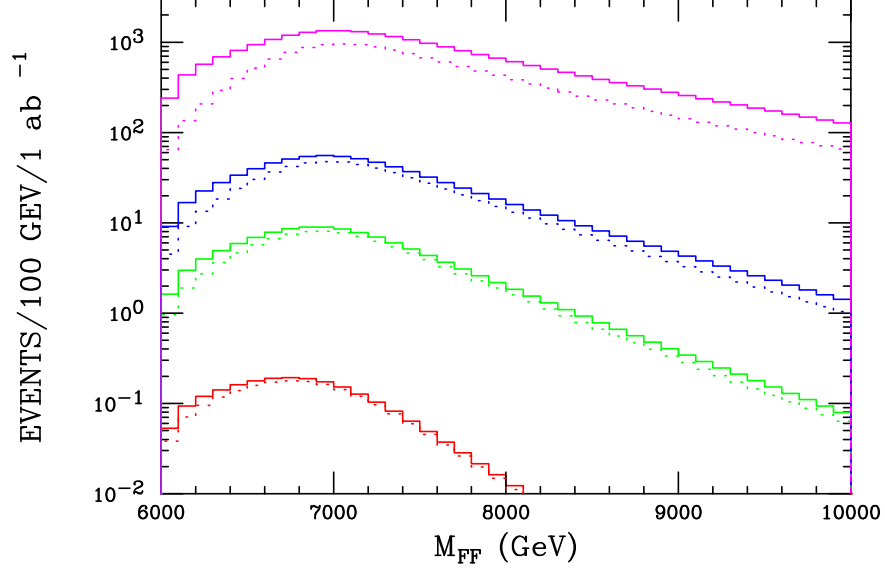


FIG. 3: Fermion KK pair production rate at various collider energies as a function of the fermion pair invariant mass assuming that the first gluon and fermion KK states are degenerate with a mass of 3 TeV. From bottom to top the histograms correspond to  $\sqrt{s} = 14, 21, 28$  and 60 TeV, respectively. No cuts have been applied. The dotted histogram shows the result of only including zero mode gluon exchange.

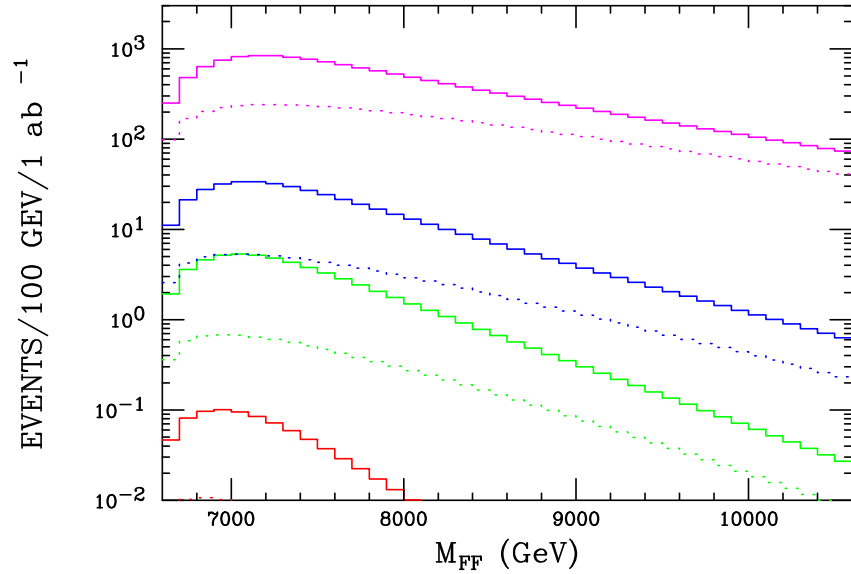


FIG. 4: Same as the previous figure but now assuming that the KK fermion is 10% more massive than the first gauge KK state.

since it involves three IR-brane states (CFT composites, in the dual picture). For example, if a singlet quark is much more UV-localized than its doublet counterpart, the doublet KK mode will decay through channel A, whereas the singlet KK mode will decay mostly through channel B (since it is more massive than the doublet KK mode). With our reference values, the singlet and doublet KK modes of light flavors are taken to be degenerate, which essentially eliminates channel B. However, this is not typically expected to be the case in a realistic setup, where doublet and singlet quarks have differing values of profile parameter  $c$ . We have also ignored the effect of mixing in the mass eigen-basis, where one expects that the degenerate KK modes are split by off-diagonal Yukawa couplings [11]. Exactly what decay modes will dominate for each quark KK state depends on the  $c$  values and possible mixing angles. Nonetheless, given the above three channels, the typical final states corresponding to the decay of the pair-produced quark KK modes are expected to be given by  $2 \times [q t \bar{t}]$ ,  $2 \times [H q t \bar{t}]$ , or  $2 \times [H H q]$ . Needless to say, these are complicated final states and require further study regarding their reconstruction and possible backgrounds.

A complete verification of WHFM, based on the RS picture, would require the observation of the first graviton KK state. This is known to be difficult at LHC energies if the gauge KK mass is 3 TeV; the graviton KK mass in this case is  $\simeq 4.7$  TeV. A promising search mode is to look for the process  $gg \rightarrow G^{(1)} \rightarrow Z_L Z_L$  [21] which is rather clean; here  $Z_L$  denotes a longitudinal  $Z$  which is IR-localized. The SM background arises from the conventional tree-level process  $q\bar{q} \rightarrow ZZ$  via  $t$ - and  $u$ - channel diagrams which is highly peaked in the forward and backward directions and is reducible by strong rapidity cuts. Note that as the  $\sqrt{s}$  of the collider increases the average collision energy also increases. This leads to a stronger peaking of the SM  $ZZ$  background in both the forward and backward directions. Since the decay products of the  $Z$ 's essentially follow those of their original parent particle a tightening of the rapidity cuts will be necessary as  $\sqrt{s}$  increases to maintain a reasonable signal to background ratio. In performing these calculations, given our assumptions, the only free parameter is the ratio  $k/\bar{M}_P$ .

Figs. 5, 6 and 7 show the results of these calculations for three different values of the ratio  $k/\bar{M}_P = 0.5, 1.0$  and  $0.1$ , respectively; as expected, in all cases the event rate is far too low at the LHC to be observable. For  $k/\bar{M}_P = 0.5$ , the graviton KK is a reasonably well-defined resonance structure which grows quite wide (narrow) when this same ratio equals 1 (0.1). For a fixed rapidity cut, the signal over the background is seen to diminish as the center

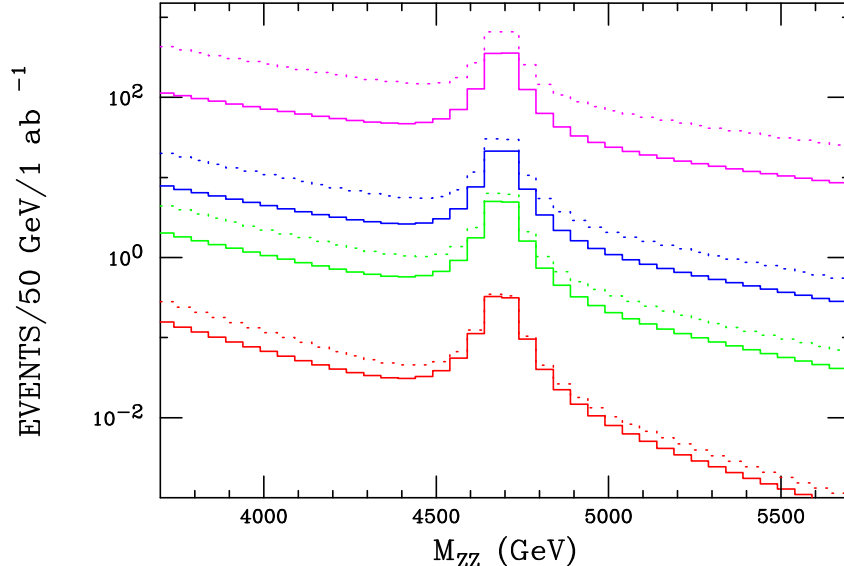


FIG. 5: Production rate for the first graviton KK excitation decaying into two  $Z$  bosons assuming a rapidity cut  $|y| < 2(1)$  on the  $Z$ 's corresponding to the dotted(solid) histograms. The histograms correspond, from bottom to top, to collider energies of  $\sqrt{s} = 14, 21, 28$  and  $60$  TeV, respectively,  $Z$  branching fractions are not included and  $k/\bar{M}_P = 0.5$  has been assumed.

of mass energy of the collider grows larger. If we identify the graviton through the decay  $ZZ \rightarrow jj\ell^+\ell^-$ , which has a branching fraction of a few percent, it is clear that a  $\sqrt{s} \sim 60$  TeV collider will be necessary to observe this state. Here, we ignore detection issues related to having collimated jets from highly boosted  $Z$ 's. A realistic jet resolution could make these conclusions less optimistic. However, we refrain from making assumptions about the detector capabilities and data analysis methods of future NHC experiments. Note that if  $k/\bar{M}_P$  is sufficiently small even this large collider energy will be insufficient as to discover the graviton KK resonance as it becomes quite narrow.

It is also of some interest to examine the possibility of searching for gluon KK states via pair production now that we are considering higher energy colliders. The production of resonant single gluon KK states is made difficult since it can only occur through the light initial state partons which have suppressed couplings to the KK gluons. The possibility of pair production avoids these issues as it arises from both  $gg$  as well as  $q\bar{q}$  initial states and occurs through the exchange of the complete gluon KK tower; we include the first three gluon KK states in the calculations below in addition to the SM gluon zero mode. Once produced, gluon KK states almost uniquely decay to top quark pairs, in typical scenarios

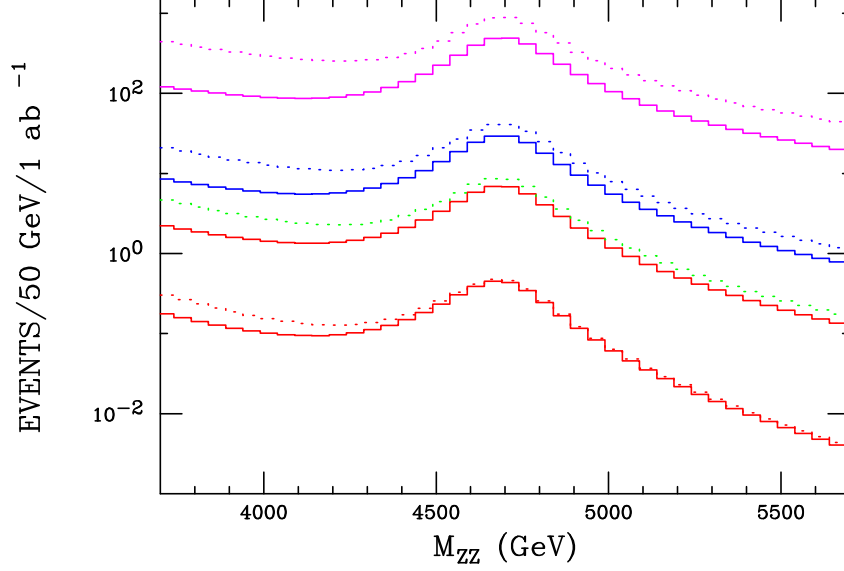


FIG. 6: Same as the previous figure but now with  $k/\bar{M}_P = 1.0$ .

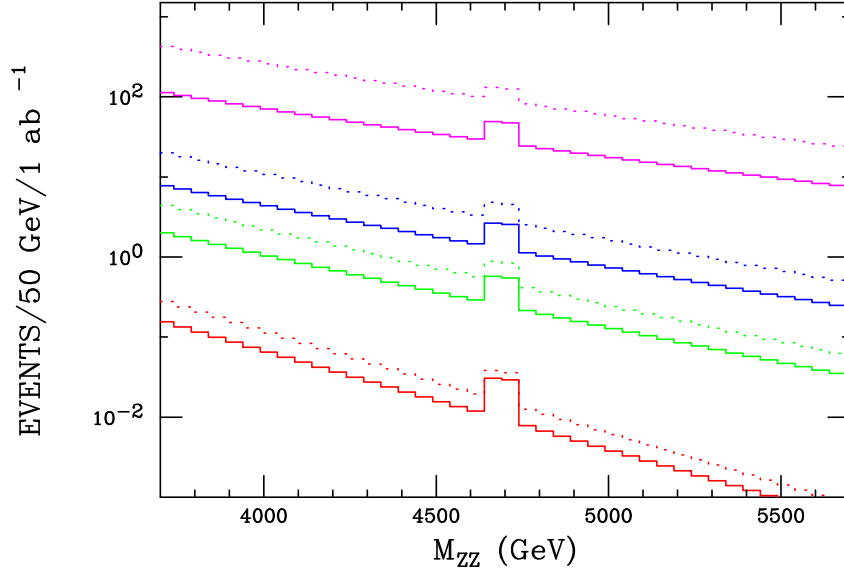


FIG. 7: Same as the previous figure but now with  $k/\bar{M}_P = 0.1$ .

[17, 18]. Since 2 KK gluon states are made, the final state consists of two pairs of top quarks.

Fig. 8 shows the results of these calculations for the same collider energies as above, *i.e.*,  $\sqrt{s} = 14, 21, 28$  and  $60$  TeV. As can be seen here, these signal rates can be quite significant once we go to energies substantially above that of the LHC. In order to determine how significant the resulting signal from these rates is we need to have an estimate of the SM background. We will not consider this background here and only provide the production

rate.

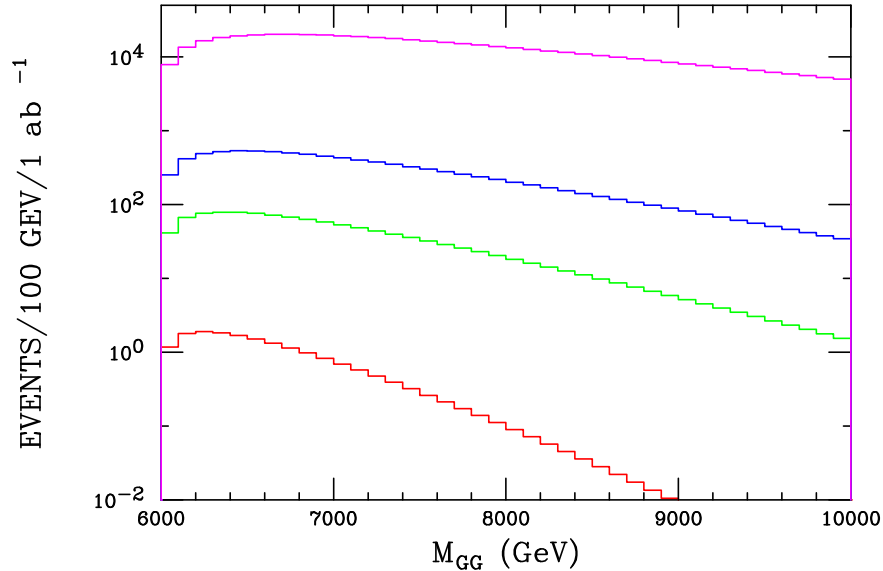


FIG. 8: Same as Fig. 3 except now for the pair production of the lightest gluon KK state.

The  $q\bar{q} \rightarrow g^{(1)} \rightarrow t\bar{t}$  gluon KK channel essentially sets the discovery reach for the RS scenario at hadron colliders [17, 18]. At the LHC, a 3 TeV KK gluon should be visible above the usual top quark pair SM background, with suitable rapidity cuts, after branching fractions and tagging efficiencies are accounted for. Unfortunately, as in the graviton KK  $ZZ$  mode above, as the center of mass energy of the collider increases the forward/backward peaked SM  $gg, q\bar{q} \rightarrow t\bar{t}$  process grows quite rapidly relative to the KK gluon signal for fixed rapidity cuts. (Recall that at these energies the decay products of the top quark will essentially follow the original top flight direction.) This result can be seen quite explicitly in Fig. 9. Here we see that the obvious gluon KK peak structure slowly disappears with increasing collider energy.

If we want to ensure a significant signal to background ratio for gluon KK states at higher energy colliders we need to tighten our rapidity cuts from the usual ‘central detector’ requirements,  $|y| < 2.5$ . In our analysis below we will assume that  $|y| < 1$  to increase the S/B ratio. Furthermore we will define the signal region to be in the  $t\bar{t}$  invariant mass range within  $\pm\Gamma_{KK}$ , the gluon KK width, of the gluon KK mass with  $\Gamma_{KK}/M_{KK} = 1/6$  assumed in our analysis below. Fig. 10 shows the resulting signal rates following this procedure for a range of KK gluon masses as a function of the collider energy; branching fractions and efficiencies have been ignored in obtaining these results.



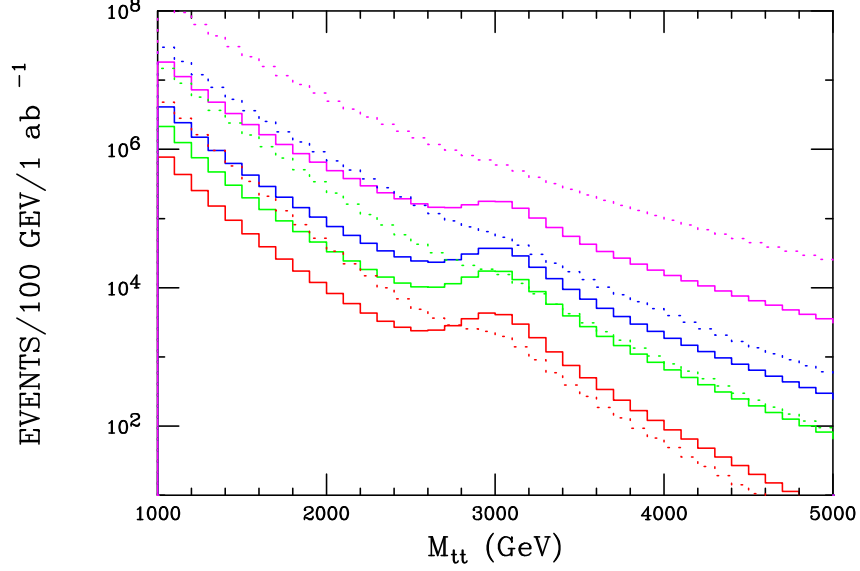


FIG. 9: The resonant production rate for the first gluon KK state in the  $t\bar{t}$  channel assuming  $|y| < 2.5$  for the dotted case and  $|y| < 1$  for the solid one. From bottom to top the histograms correspond to  $\sqrt{s} = 14, 21, 28$  and  $60$  TeV respectively. No efficiencies or branching fractions are included.

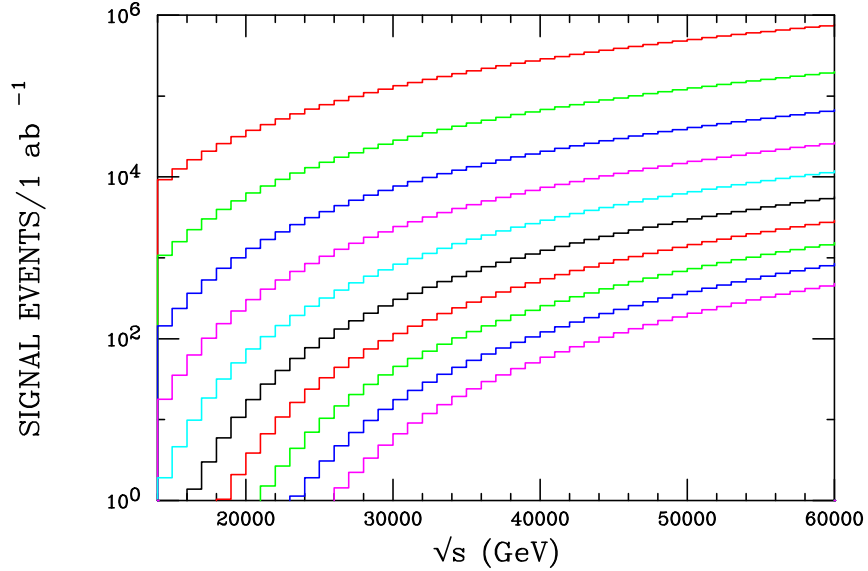


FIG. 10: Signal rate for a possible gluon KK resonance as a function of the collider energy employing the cuts described in the text. Branching fractions and efficiencies have been neglected. From top to bottom the results are shown for gluon KK masses in the range from 3 to 12 TeV in steps of 1 TeV.

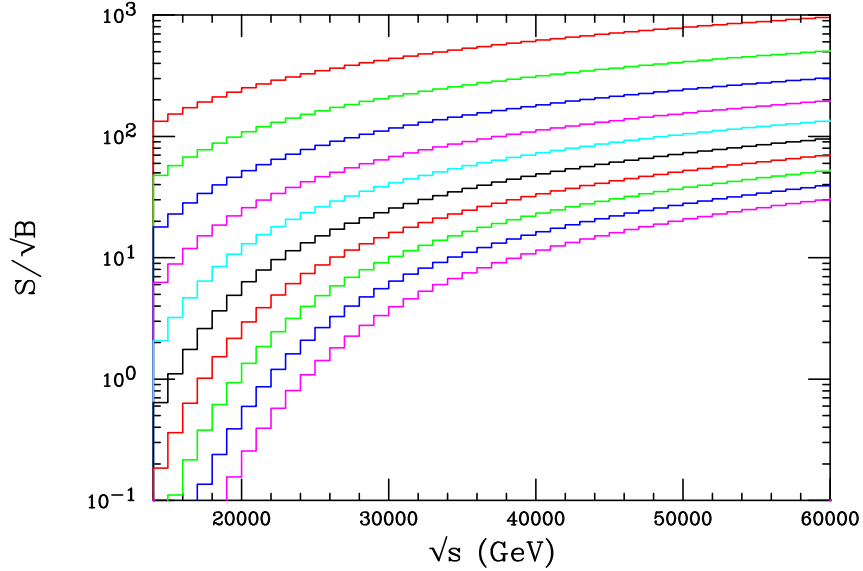


FIG. 11: Same as the previous figure but now showing the signal significance. Again, branching fractions and efficiencies have been neglected.

Fig. 11 shows the signal significance for gluon KK production for a range of masses as a function of the hadron collider center of mass energy. In a more realistic calculation which includes top quark branching fractions  $f$  and  $b$ -tagging efficiencies  $\epsilon$ , the results shown here must be scaled by  $\sqrt{f\epsilon} \sim 0.15$  [17]. Taking this factor into account we see that, *e.g.*, at a  $\sqrt{s} = 21$  (28, 60) TeV collider KK gluon masses as large as 5.5 (7, 12) TeV may become accessible. One could say that this covers the entire ‘natural’ parameter space for WHFM.

#### IV. CONCLUSIONS

Amongst models of physics beyond the Standard Model, WHFM are rather unique to the extent that they are capable of providing a simultaneous natural resolution of two important puzzles, namely the hierarchy and the flavor problems. In particular, this is in sharp contrast to supersymmetry, which is otherwise an extremely interesting theoretical construct.

Thus, it is clearly important to establish the requirements for direct experimental verification of WHFM. These more recent developments of the original RS model [1], which explain gauge and flavor hierarchies in one framework, have KK particles in the few TeV range. Low energy precision tests suggest that gauge KK masses in WHFM are likely to be heavier than about 3 TeV. Perhaps the most compelling and unique signature of these models is the

spin-2 KK graviton. Unfortunately, it seems at the LHC, even with an upgraded luminosity, KK gravitons, expected here to lie above 4.7 TeV, are very challenging to observe and likely inaccessible. Prospects for KK gluons up to masses around 4 TeV seem brighter at the LHC. Thus it may well be that some early indication of the underlying RS idea may find support at the LHC. However, though considerable work exists in the literature on warped *bosonic* KK modes, not much has been done for the SM fermion counterparts. The observation of these *fermionic* KK modes can in essence be taken as direct experimental evidence for warped bulk flavor.

With that perspective in mind, in this work, we set out to provide an exploratory study of the parameters needed for the next generation of machines that could provide significant experimental support for the WHFM, and especially for generation of flavor through bulk localization. We concentrate on hadron colliders only, as they are expected to yield the largest kinematic reach. For definiteness, throughout our numerical study here, we take the lightest gauge KK mass to be 3 TeV; SM fermionic KK modes are always as massive or heavier.

First, we studied single KK fermion production. The most promising candidate in this regard is the KK mode of the third generation doublet produced in association with a  $t$  or a  $b$  quark. We found that at the LHC the prospects for finding this KK fermion through single production are rather grim. In fact, we showed that even a 28 TeV machine is only likely to see at most a handful of candidate events of this category. The prospects improve significantly for a 60 TeV machine wherein a few tens of events are possible.

Pair production of KK fermions typically seems to have over an order of magnitude larger cross section compared to the single-production, for large  $\sqrt{s}$ . For pair production, a 28 TeV machine can give several tens of events and 60 TeV produces hundreds of such candidate events. One may expect that a sample of this latter size is needed for a reliable verification of the bulk flavor scenarios, after cuts and efficiencies are taken into account; we do not delve into these issues in this exploratory work.

We have revisited the earlier study of the KK graviton through the “gold plated”  $ZZ$  mode [21]. We find that for this unique channel, only a 60 TeV machine can provide  $\mathcal{O}(100)$  events over a plausible range of  $k/\bar{M}_P$  values. Thus, it seems that verification of the WHFM, in the sense of directly measuring the properties of signature KK modes, requires what we refer to as the Next Hadron Collider (NHC) with  $\sqrt{s} \approx 60$  TeV and  $\mathcal{O}(1)$   $\text{ab}^{-1}$  of integrated

luminosity. We have also extended earlier studies of the resonance production of the first KK gluon state and its detection through a  $t\bar{t}$  pair. We find that colliders with energies 14, 21, 28 and 60 TeV can allow detection of the first KK gluon up to masses 4, 5.5, 7, and 12 TeV, respectively.

We hence conclude that an NHC-class machine must be an integral part of the high energy experimental program if hints of WHFM are discovered at the LHC. The same conclusion holds for 4D models that explain hierarchy and flavor in a similar fashion and constitute dual dynamical scenarios, according to AdS/CFT correspondence [24, 25].

### Acknowledgments

H.D. and A.S. are supported in part by the DOE grant DE-AC02-98CH10886 (BNL).

- 
- [1] L. Randall and R. Sundrum, Phys. Rev. Lett. **83**, 3370 (1999) [arXiv:hep-ph/9905221].
  - [2] W. D. Goldberger and M. B. Wise, Phys. Rev. Lett. **83**, 4922 (1999) [arXiv:hep-ph/9907447].
  - [3] H. Davoudiasl, J. L. Hewett and T. G. Rizzo, Phys. Rev. Lett. **84**, 2080 (2000) [arXiv:hep-ph/9909255].
  - [4] W. D. Goldberger and M. B. Wise, Phys. Rev. D **60**, 107505 (1999) [arXiv:hep-ph/9907218].
  - [5] H. Davoudiasl, J. L. Hewett and T. G. Rizzo, Phys. Lett. B **473**, 43 (2000) [arXiv:hep-ph/9911262].
  - [6] A. Pomarol, Phys. Lett. B **486**, 153 (2000) [arXiv:hep-ph/9911294].
  - [7] Y. Grossman and M. Neubert, Phys. Lett. B **474**, 361 (2000) [arXiv:hep-ph/9912408].
  - [8] T. Gherghetta and A. Pomarol, Nucl. Phys. B **586**, 141 (2000) [arXiv:hep-ph/0003129].
  - [9] M. S. Carena, E. Ponton, J. Santiago and C. E. M. Wagner, Phys. Rev. D **76**, 035006 (2007) [arXiv:hep-ph/0701055].
  - [10] K. Agashe, G. Perez and A. Soni, Phys. Rev. D **71**, 016002 (2005) [arXiv:hep-ph/0408134].
  - [11] K. Agashe, A. E. Blechman and F. Petriello, Phys. Rev. D **74**, 053011 (2006) [arXiv:hep-ph/0606021].
  - [12] K. Agashe, A. Delgado, M. J. May and R. Sundrum, JHEP **0308**, 050 (2003) [arXiv:hep-ph/0308036].

- [13] K. Agashe, R. Contino and A. Pomarol, Nucl. Phys. B **719**, 165 (2005) [arXiv:hep-ph/0412089].
- [14] K. Agashe, R. Contino, L. Da Rold and A. Pomarol, Phys. Lett. B **641**, 62 (2006) [arXiv:hep-ph/0605341].
- [15] C. Dennis, M. K. Unel, G. Servant and J. Tseng, arXiv:hep-ph/0701158.
- [16] K. Agashe, A. Delgado, M. J. May and R. Sundrum, JHEP **0308**, 050 (2003) [arXiv:hep-ph/0308036]; K. Agashe, R. Contino, L. Da Rold and A. Pomarol, Phys. Lett. B **641**, 62 (2006) [arXiv:hep-ph/0605341].
- [17] K. Agashe, A. Belyaev, T. Krupovnickas, G. Perez and J. Virzi, arXiv:hep-ph/0612015.
- [18] B. Lillie, L. Randall and L. T. Wang, arXiv:hep-ph/0701166.
- [19] K. Agashe *et al.*, arXiv:0709.0007 [hep-ph].
- [20] A. L. Fitzpatrick, J. Kaplan, L. Randall and L. T. Wang, arXiv:hep-ph/0701150.
- [21] K. Agashe, H. Davoudiasl, G. Perez and A. Soni, Phys. Rev. D **76**, 036006 (2007) [arXiv:hep-ph/0701186].
- [22] H. Davoudiasl, J. L. Hewett and T. G. Rizzo, Phys. Rev. D **63**, 075004 (2001) [arXiv:hep-ph/0006041].
- [23] H. Davoudiasl and A. Soni, arXiv:0705.0151 [hep-ph].
- [24] J. M. Maldacena, Adv. Theor. Math. Phys. **2**, 231 (1998) [Int. J. Theor. Phys. **38**, 1113 (1999)] [arXiv:hep-th/9711200].
- [25] N. Arkani-Hamed, M. Porrati and L. Randall, JHEP **0108**, 017 (2001) [arXiv:hep-th/0012148]; R. Rattazzi and A. Zaffaroni, JHEP **0104**, 021 (2001) [arXiv:hep-th/0012248].